



# Bulletin of the Mineral Research and Exploration

<http://bulletin.mta.gov.tr>



## Geological structures mapping using aeromagnetic prospecting and remote sensing data in the karstic massif of Beni Mellal Atlas, Morocco

Ikram BOUTIRAME<sup>a\*</sup>, Ahmed BOUKDIR<sup>aID</sup>, Ahmed AKHSSAS<sup>bID</sup> and Ahmed MANAR<sup>cID</sup>

<sup>a</sup>Sultan Moulay Slimane University, Faculty of Sciences and Technics, Department of Geology, Post box 523, Beni Mellal/Morocco.

<sup>b</sup>Mohamed 5 University, Mohammadia School of Engineers, Laboratory of Applied Geophysics, Geotechnics, Engineering Geology and Environment, Post box 765, Agdal, Rabat/Morocco.

<sup>c</sup>Ministry of Energy, Mines and sustainable development, Postbox 6208, Agdal, Rabat/Morocco.

Research Article

### Keywords:

Beni Mellal Atlas,  
Aeromagnetic data,  
Sentinel-1, Lineaments.

### ABSTRACT

The current study exposes the results of aeromagnetic data interpretation and a combined analysis of 1-A sentinel radar image that cover the study area of Beni Mellal Atlas in order to describe the structural geometry and to understand its tectonic evolution. The map of the reduced to pole of residual magnetic field highlights various magnetic anomalies with high amplitudes that correspond to Jurassic-Cretaceous basaltic formations outcropping synclinal basins of Beni Mellal Atlas. The interpretation of magnetic data using tilt derivative (TDR), horizontal gradient technique coupled to upward continuation and Euler Deconvolution allows us to distinguish the fractures network that is affecting the study area. In order to complete this analysis, the Sentinel-A radar image is processed and filtered using SNAP ESA Sentinel-1 toolbox software to extract lineaments. The final structural map reveals four faults groups oriented respectively NE-SW, ENE-WSW to E-W, N-S and NW-SE. Their depths estimated by the application of Euler deconvolution exceed 1500 m. These faults have played a major role in structural evolution of Beni Mellal Atlas.

Received Date: 18.06.2018

Accepted Date: 23.12.2018

## 1. Introduction

The detection of geological lineaments such as faults, fractures, lithological contacts...etc., is a crucial step for the success of hydrogeological and mining research studies. These linear structures may contain mineralization or constitute potential pathways for groundwater flow, particularly in the karstic area (Khamis et al., 2014; Dauteuil et al., 2016). The karstic massif of Beni Mellal, which is the object of this study, is a bordering mountain range where the rise of the carbonate rocks overlooks Tadla plain from 2400 m (Benzaquen, 1963; Rolley, 1973; Monbaron, 1982). The Beni Mellal Atlas –Tadla plain junction zone, known as the Beni Mellal Dir, is a highly undulating zone with steep-slope valleys (Benzaquen,

1963) and is characterized by a dense vegetation cover that hides the geological formations and obstructs the discrimination of fracture network. It is therefore necessary to use indirect methods such as remote sensing and geophysical prospecting to overcome these difficulties.

Remote sensing is widely used in geological and structural mapping (Srivastava and Bhattacharya, 2006; Alonso-Contes, 2011; Adiri et al., 2017). The use of this technique becomes more effective when combined with complementary data such as geophysical. In fact, remote sensing can extract multitude of data about the structure and composition of the Earth's surface using satellite image acquisition and interpretation processes. The radar images provide

Citation info: Boutirame, I., Boukdir, A., Akhssas, A., Manar, A. 2019. Geological structures mapping using aeromagnetic prospecting and remote sensing data in the karstic Massif of Beni Mellal Atlas, Morocco. Bulletin of the Mineral Research and Exploration, 160, 213-229. <http://dx.doi.org/10.19111/bulletinofmre.502094>

\* Corresponding author: Ikram BOUTIRAME, [i.boutirame@usms.ma](mailto:i.boutirame@usms.ma)

the information on the subsoil roughness and texture and highlight the relief of the structural discontinuities. Thus, they have a strong potential for the geological studies and in particular structural evaluations owing to their independence to environmental conditions (e.g. climatic conditions, density of vegetation cover, rugged topography ...).

Numerous studies have been carried out using radar remote sensing tools in structural mapping (Mansour and Ait Brahim, 2005; Corgne et al., 2010). In Morocco, Adiri et al. (2017) have made a comparison between remote sensing data multi-sources (optical and radar remote sensing) for automatic lineaments extraction in the region of Sidi Flah-Bouskour inlier, Anti-Atlas Morocco. Because of its high sensitivity to geomorphology, the Sentinel-1 radar sensor gives better results than optical sensors. In reality, each geological formation is characterized by a particular radar texture that corresponds to a defined magnetic, gravimetric or electrical anomaly. The synergy of geophysical data and radar images makes it possible to gather precise geological informations to determine the fractures network (Ranganai et al., 2008; Megwara et al., 2014; Ejep et al., 2017; Boutirame et al., 2018).

The aim of this study is the lineament mapping in the Beni Mellal Atlas based on the combination of airborne magnetic data and Sentinel-1 image interpretation. The fractures deduced from this study checked against field measurements and observations to characterize its spatial distribution in the study area on the one hand, and to be able to understand its structural and geological origin on the other hand.

### 1.1. Description of Study Area

#### 1.1.1. General Context

The Beni Mellal Atlas, the subject of this study, corresponds to the north occidental edge of the central High Atlas (Rolley, 1973). It is located in the south of Tadla plain, outskirts of the junction between High and Middle Atlas. Its highest point is R’Nim mountain that reaches 2411m above sea level (Figure 1a and b). A decrease in altitude is observed from south to north, it moves up from 1000 m (El Ksiba) on the edge of the Atlas to less than 500 m in Tadla plain. The karstic massif of Beni Mellal Atlas is formed; essentially; by fractured carbonate deposits of Lower and Middle Jurassic, constituting the main outcrops of the mountainous area that overhangs Beni Moussa

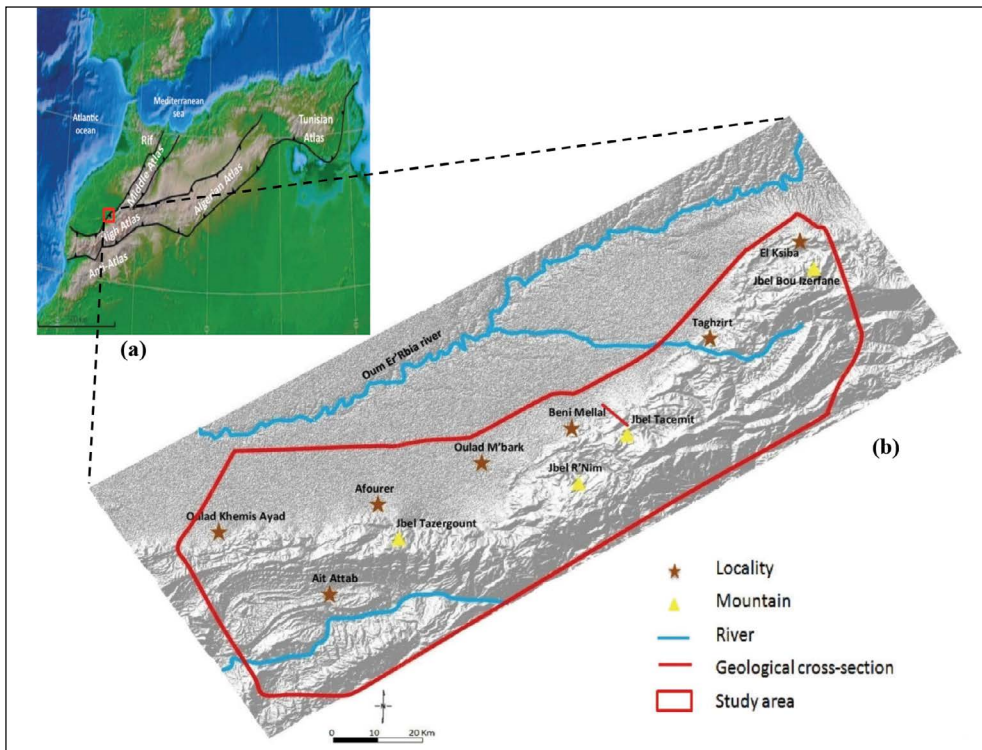


Figure 1- a) Map of North Africa showing the location of the study area on digital topography; b) Shaded relief of Sentinel-1A image showing the study area limits.

plain. Those formations carried in altitudes, present typical karst forms such as dolines, avens, caves and sinkholes (Bouchaou, 1988).

1.1.2. Geological Setting

The Beni Mellal Atlas is an open and flattened anticline that abruptly dominates Beni Moussa plain through a fault system, the most important one is the North Atlasic Fault (Tadla overlap). It is the key area of Central High Atlas (Guezal et al., 2013), its geological history is therefore linked to this intracontinental chain (Michard, 1976; Mattauer et al., 1977; Ziegler et al., 1995), whose various structural elements are a result of geodynamic evolution that began with distal tectonics at the end of Paleozoic and during Mesozoic by the opening of Tethys sea (Du Dresnay, 1972; Laville and Harmand, 1982; Beauchamp, 1988 and Piqué et al., 1998). Its northern border is characterized by a succession of overlapping structural units that rest on the Liassic and Tertiary

thrusts of Dir (Figure 2c). The Mesozoic formations consist of massive carbonates of Lower and Middle Jurassic, detrital Bathonian-Early Cretaceous deposits (“red-layer” formations), and Cretaceous carbonates and terrigenous deposits (Figure 2a).

The Mesozoic serie rests on a Paleozoic basement deformed during the Hercynian orogeny (Hoepffner et al., 2006). It begins with Triassic rocks formed of red clays with basaltic intercalations. The Lower and Middle Lias consist of bedded limestones and dolomites surmounted by chocolate marls of Toarcian-Aalenian age. The Upper Jurassic and Lower Cretaceous are characterized by red detrital deposits known in the literature as «red beds» (Souhel, 1996; Haddoumi, 1988). This “red beds” formation is composed of three lithostratigraphical units forming large basins (Jenny et al., 1981). We distinguish from bottom to top: Guettioua formation, Iouaridene formation and detrital deposits of Jbel Sidal formation (Charrière et al., 2005; Haddoumi et al., 2010 ). This

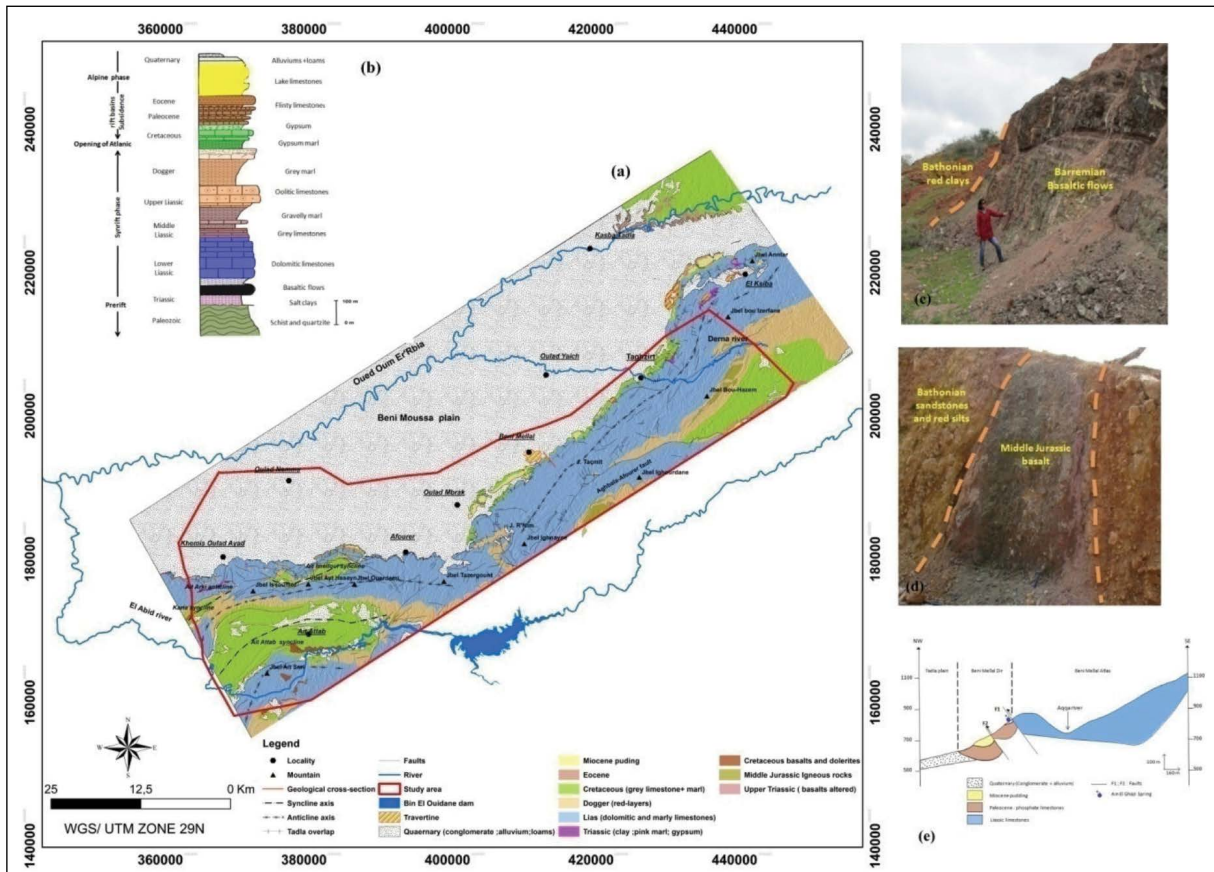


Figure 2- a) Geological map of the study area (Benzaquen, 1963; Monbaron, 1985 and Verset, 1985), b) Litho-stratigraphic log of Beni Mellal Atlas, c) Pictures showing basaltic flows in Beni Mellal Atlas, d) NW-SE geological cross-section showing the different units of the study area: Tadla plain, piemont and mountainous zone of Beni Mellal Atlas.

important detrital deposit has been accompanied by Jurassic-Cretaceous magmatic occurrences. The latter, outcrop in the synclinal basins of Beni Mella (Guezal et al., 2013 ) represented as two successive horizons interbedded in the sandstone-detrital series of “red beds” (Jenny et al., 1981; Haddoumi, 1988; Souhel, 1996) (Figure 2b):

- Basaltic horizon B1: outcrops on the northern flank of Ait Attab syncline. This basaltic complex consists of volcanoclastic deposits placed in the upper part of Guettioua formation (Michard et al., 2011);
- Basaltic horizon B2: is associated with the base of Jbel Sidal formation and thicker compared to the previous one, this second episode is effected during the Barremian with the form of three massive flows separated by red clays (Bardon et al., 1978; Souhel, 1996).

The Tertiary serie is presented by phosphated limestones and Maestrichtian-Paleocene marls. The Mesozoic and Tertiary cover is unconformably capped by Mio-Pliocene lake limestones and Quaternary alluviums (Jabour and Nakayama, 1988; Beauchamp, 1988). The mainly carbonate marine sedimentation during the lower and middle Lias and the detrital deposits during the lower Bathonian-Cretaceous (Souhel, 1987; Haddoumi, 1988) were controlled by a tectonics extension oriented NW-SE. Indeed, during the lower and middle Lias two major faults were active: the Beni Ayat border fault and the Ait Seri fault which delimits in the north the Ait Seri block (Figure 3) where a reef-facies carbonate platform is deposited. The Toarcian's marly deposits obscure the Ait Seri fault, and at the same time the tectonic activity is transferred to another fault called Karia fault that appears between the Karia and Ait Imelloul blocks. The distensive synsedimentary tectonics continues with the appearance of “Issoumer fault” bordering and tipping the Ait Attab block to the west (Figure 3).

## 2. Data and Method

### 2.1. Aeromagnetic Data Processing

The airborne magnetic data, which is used in this study, was obtained from the Ministry of Mines and Energy of Rabat in form of two residual magnetic field maps with a scale of 1: 100,000 (Beni Mellal

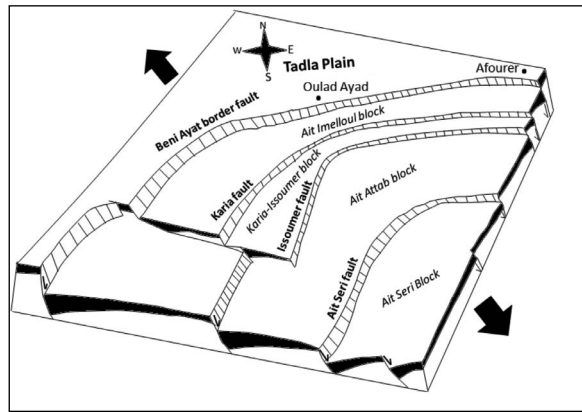


Figure 3- Schematic model showing the paleogeography of Ait Attab region during Jurassic.

and Afouerer sheets). These data result from an aeromagnetic study carried out in the Central High Atlas by the African Geophysical Company in 1970. The data was acquired by a magnetic equipment type C.S.F Caesium Steamer on board a plane type 680 FL. At a barometric altitude of 2600 m, the aeromagnetic survey carried out consisted of flight lines oriented NW-SE and spaced 3.5 to 4 km apart, and transverse lines oriented NE-SW with 10 to 15 km spacing. The two residual magnetic field maps were scanned and digitized using ArcGIS software, then processed by applying several mathematical filters and transformation operators using Geosoft Oasis Montaj software (version 8.3) namely the horizontal gradient, Tilt-Derivative and Euler Deconvolution. The application of these filters has allowed the elaboration of several maps, which we refer to in the review and structural interpretation of the magnetic results.

#### 2.1.1. Residual Magnetic Field and Reduction to the Pole (RTP)

The residual magnetic field map (Figure 4) highlights the existence of magnetic maxima and minima showing important variation of the magnetization in the subsoil with magnetic field values oscillating between 960 and 1064 nT. In order to better visualize these magnetic anomalies and to facilitate the analysis and the structural interpretation of results, the residual aeromagnetic field has been reduced to pole (RTP). This reduction makes it possible to eliminate the anomalies distortion caused by inclination of the earth's magnetic field (El Gout et al., 2009) by transforming the magnetic anomaly as if it were located at the north magnetic pole and to



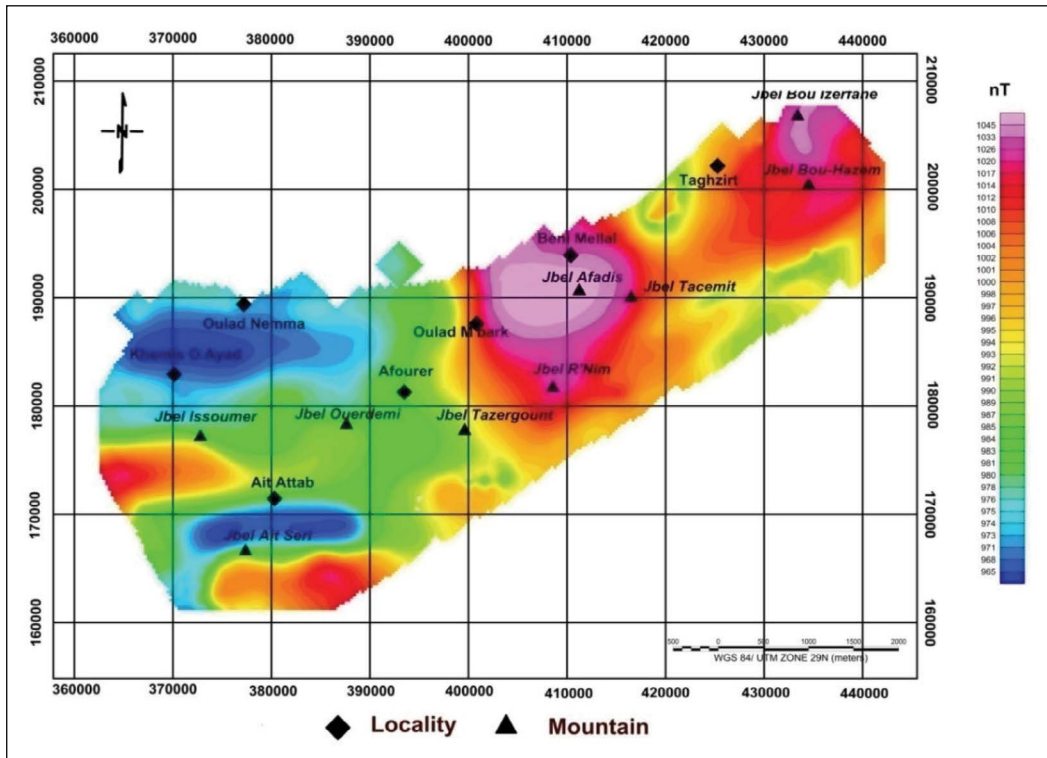


Figure 4- Residual magnetic field of the study area.

replace back anomalies on the apex of the sources that create them, provided that the magnetization is not remanent (Debeglia, 2005).

The analysis of (Figure 5) the reduced to the pole residual magnetic map reveals the existence of several magnetic anomalies of different shapes and amplitudes. It shows high magnetic responses in the center, South-West and the north-east extremity of the study area (P1, P2, P3, P4, P5, and P6), while the low magnetic anomalies (N1 and N2) in blue and green colors are observed in the western and eastern parts of Beni Mellal Atlas.

### 2.1.2. Tilt Angle Transformation “Tilt-Derivative” (TDR)

In order to obtain as much information as possible from initial aeromagnetic data, we applied the Derivative Tilt Operator (TDR) (or Tilt angle) using the following geomagnetic field elements: inclination  $I = 45^{\circ}14'$  north and declination  $D = 7^{\circ}12'$  west, corresponding to aeromagnetic survey that dates from October 1975. The usefulness of this transformation operator lies in the fact that it enhances all the magnetic anomalies either with small or large amplitudes (Miller

and Singh, 1994; Salem et al., 2008). It calculates the arctangent of the ratio of vertical derivative to total horizontal derivative of the magnetic field  $T$  (Salem et al., 2008). The equation of this transformation is as follows:

$$\Theta = \tan^{-1} \left[ \frac{\frac{\delta T}{\delta Z}}{\sqrt{\left(\frac{\delta T}{\delta x}\right)^2 + \left(\frac{\delta T}{\delta y}\right)^2}} \right] \quad (1)$$

The map of the reduced residual magnetic field transformed by the method of “Tilt Derivative” (Figure 6) facilitates the structural interpretation of magnetic data and makes it possible to locate the linear structures such as the faults (Amar et al., 2012 and Amar, 2013). Indeed, the zero contours lines of TDR filter ( $\theta = 0$ ) mark the abrupt change between two different magnetic sources which consequently correspond to the contact between these sources.

### 2.1.3. Boundary Analysis Method: Horizontal Gradient

With the objective of better exploit this magnetic data and to highlighting the different structural axis that defines the deep structure of the study area,

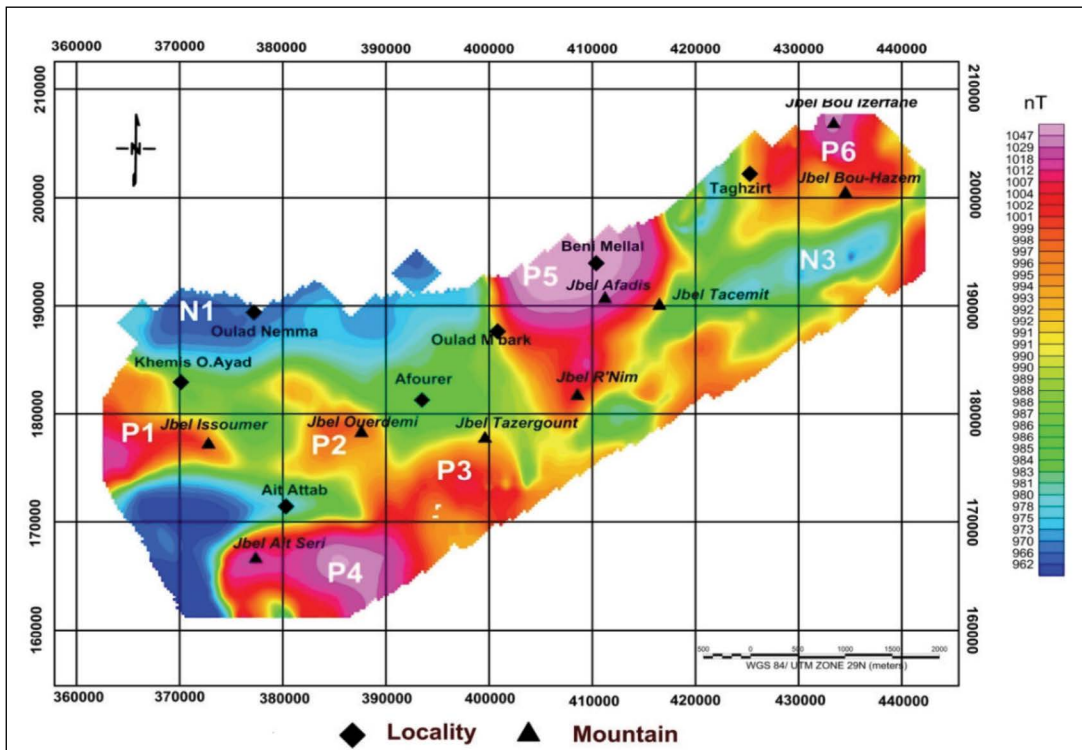


Figure 5- Reduced to pole of residual magnetic field map.

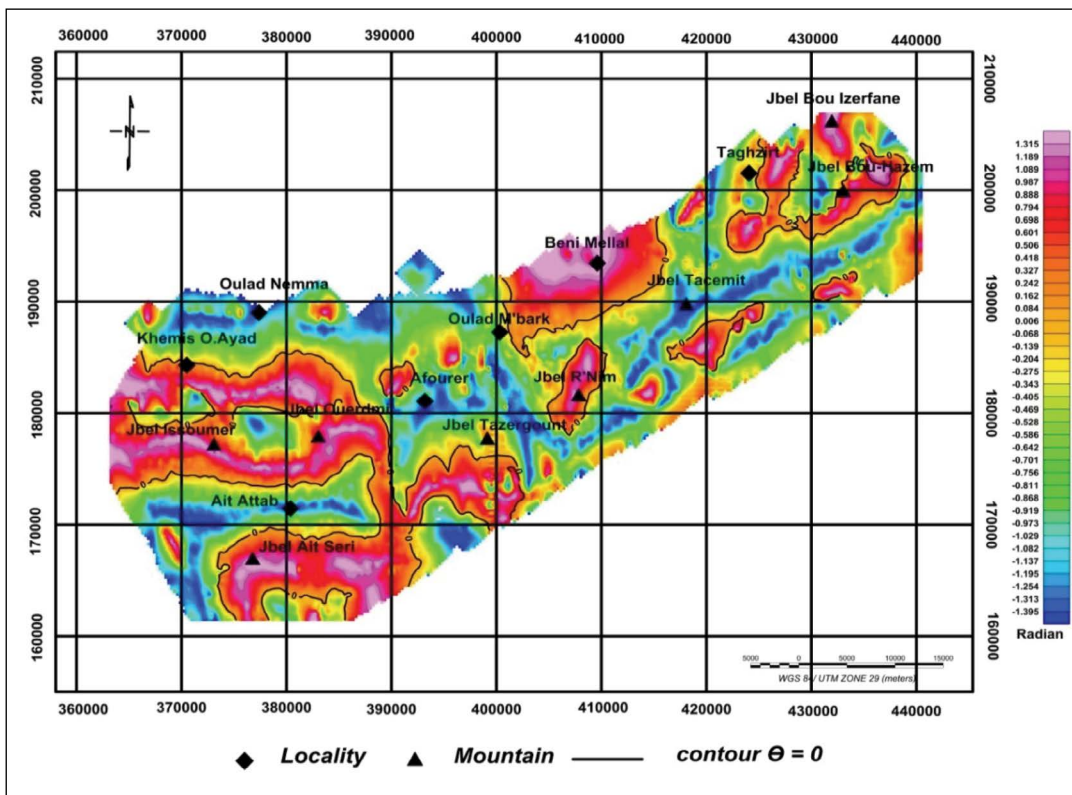


Figure 6- Tilt-Derivative magnetic map.

we have applied a multi-scale analysis method of magnetic contacts, based on, the joint use of horizontal gradient and the upward continuation techniques. This method, used by several authors (Everaerts and Mansy, 2001; Abderbi and Khattach, 2011), allows on one hand to locate the zones with rapid variation of the magnetic field caused by the lithological change or the presence of geological discontinuities (fractures, faults...), and determine the dip direction of those geological structures on the other hand. Indeed, the magnetic anomalies correspond to inflection points which transform after the horizontal gradient calculation into local maxima. These maxima are located above the geological contacts that present magnetic susceptibility contrasts (Van Senden et al., 1990). In order to determine the dip direction of those structures, a series of upward continuation has been carried out at different altitudes. For each level the horizontal gradient of the residual magnetic field is calculated and its local maxima are determined. If the structures are vertical, the maxima obtained at each altitude are superimposed. However, their migration with the upwards continuation indicates the dip direction (Figure 7).

2.1.4. Euler Deconvolution

The Euler Deconvolution method was used to estimate the location of anomalous sources on the horizontal plane and their depths (Thompson, 1982; Reid et al., 1990; Moreau et al., 1996). This technique is based on the resolution of the Euler homogeneity equation (1) using the structural index N (Reid et al., 1990) which measures the rate of potential field changes. This index varies as a function of the geometry of the detected source (Oruç and Selim, 2011).

$$(x-x_0) \left(\frac{dM}{dx}\right) + (y-y_0) \left(\frac{dM}{dy}\right) + (z-z_0) \left(\frac{dM}{dz}\right) = N*(B-M) \quad (1)$$

Where (x0, y0, z0) are the coordinates of the magnetic source, M represents the total field measured at (x,y,z), B is the regional value of the total field and N indicates the structural index.

In the current study, we applied the Euler Deconvolution method to the residual magnetic field reduced to pole using a structural index equal to zero (N = 0) with a window size of 10\*10 and a maximum

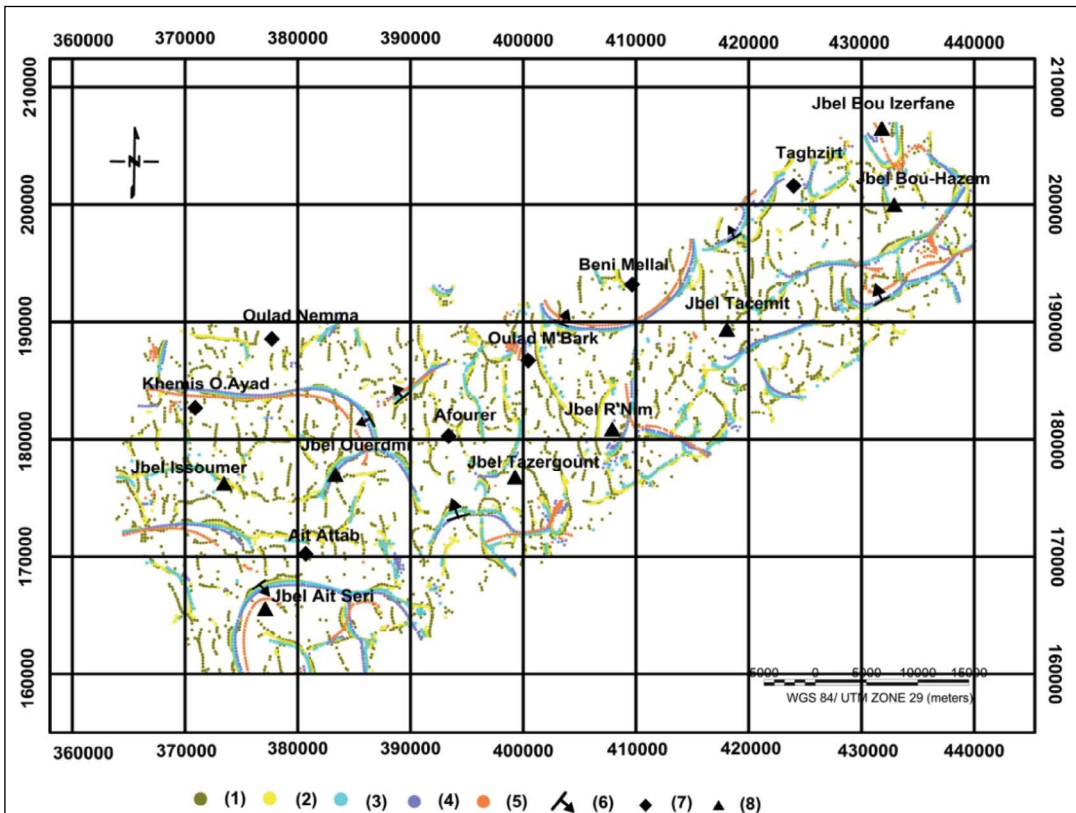


Figure 7- Superposition of the horizontal gradient maxima and its upward continuations at different altitudes: 1) 0 m; 2) 500 m; 3) 1 km; 4) 2 km; 5) 4 km. 6) dipping direction; 7) locality; 8) mountain.

relative error of 15%. A digital Elevation Model was used to remove the Euler solutions whose elevation is higher than the altitude ground.

### 2.2. Remote Sensing Data Processing

To achieve our objective, a Sentinel-1A radar image is used in this study. This image was acquired on 2 April 2017 in C-band ( $\lambda = 5.66$  cm) (Table 1). It was processed and analyzed by a free and open source software “SNAP ESA Sentinel-1 toolbox SITBX”. It is available on the official website of European Space Agency ESA.

Table 1- Sentinel-1A image characteristics.

Radar image	Sentinel-1A data
Acquisition time	02 April 2017
Acquisition orbit	Descending
Polarization	C-band (5.4GHz)
Polarization	VV-VH
Data product	Level-1 GRD

The raw radar image has undergone preliminary processing that consists of radiometric, atmospheric and geometric correction to mitigate the atmospheric effects and topographic disturbances affecting the

recorded information quality (Corgne et al., 2010). Thereafter, a “refined Lee” filter has been applied to the radar image to eliminate the flicker effect (speckle reduction) (Lee et al., 1999). For improving the lineaments perception; spatial filters were applied to the pre-treated radar image as per the four main directions N-S; NE-SW; NW-SE and E-W (Figure 8).

The interpretation and extraction of lineaments was done visually (manual extraction). Indeed, Hobbs, 1912 described the lineaments as any significant line that reveals the hidden architecture of the subsoil and having a well-defined structural signification. In our study, the lineaments location is mainly identified by their effect on the landscape (Lachaine, 1999), a change in texture or geometric shape or else by the hydrographic network disturbance. To avoid taking into consideration all linear structures with anthropogenic origin (crest line, road, paths, electrical power lines,, cultivated areas, etc.), the processed radar image has been superimposed with the topographic and land cover maps of the study area to eliminate them during the lineaments extraction. The figure 9 shows the visual interpretation results of Sentinel-1 image.

The analysis of this map shows a difference in the lineament distribution in the study area. Indeed, the

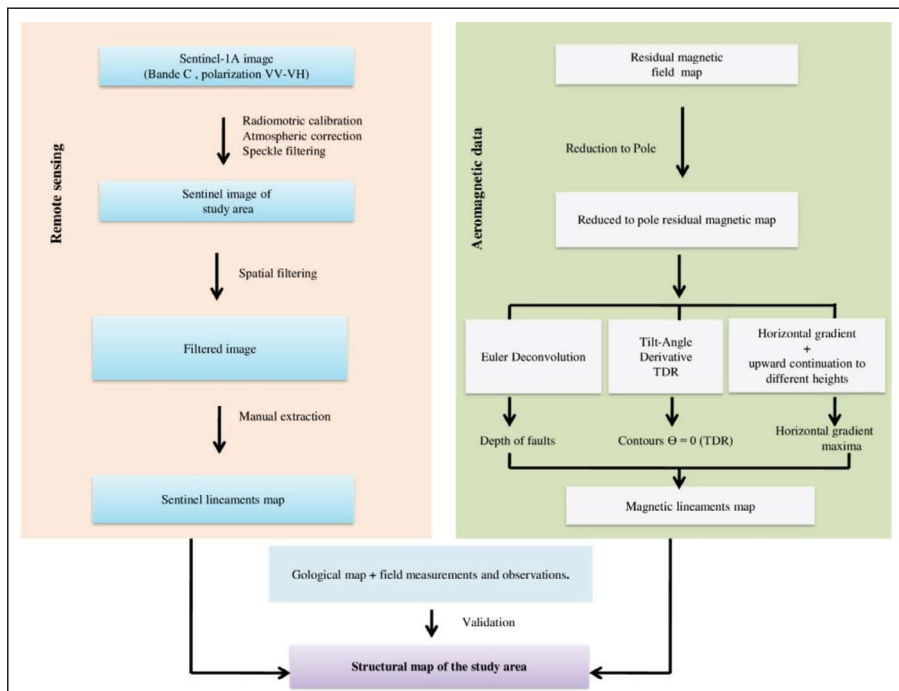


Figure 8- Flowchart of adopted methodology for lineament mapping.



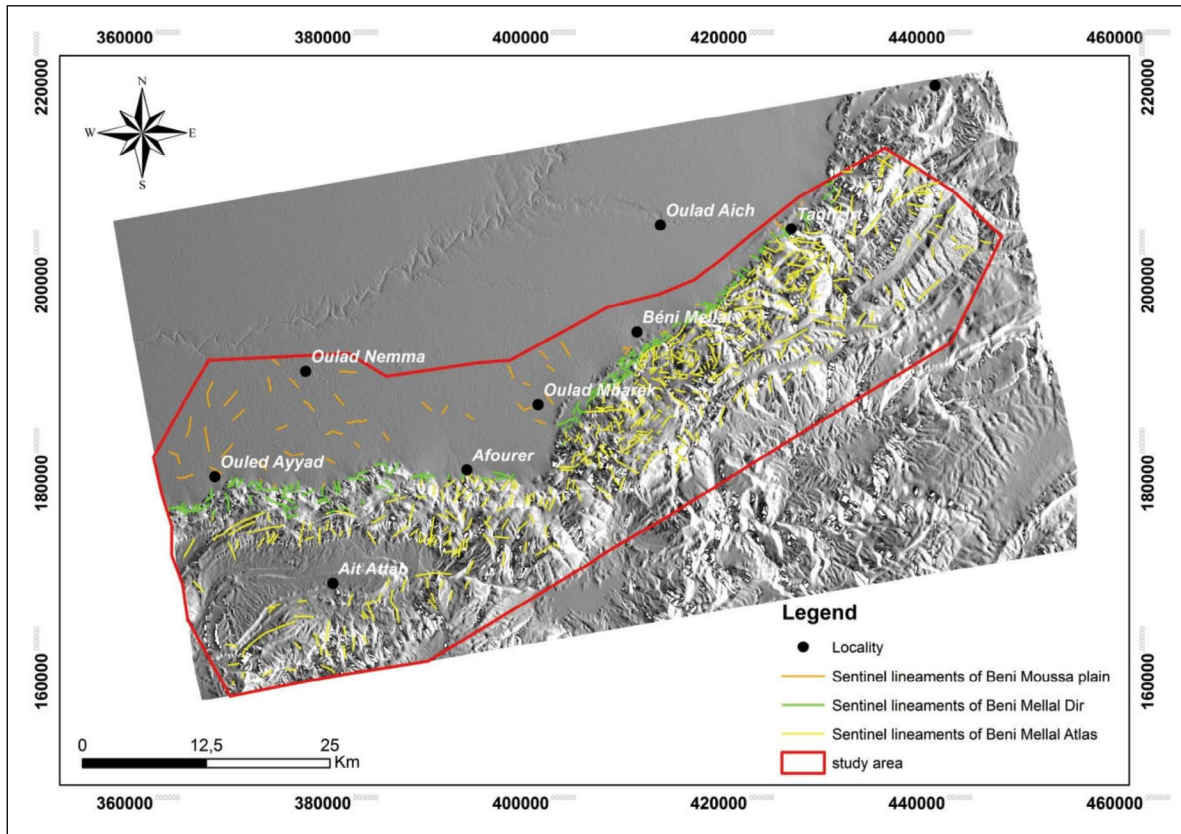


Figure 9- Extracted lineaments from processing Sentinel-1 image (Boutirame et al., 2018).

fracture density becomes more important when we go from the Beni Moussa plain towards the mountainous area of Beni Mellal Atlas. This latter presents a high lineament density with a predominance of NE-SW to ENE-WSW trending. This is related to the dolomitic and limestone nature of the Jurassic formations that occupy the totality of Beni Mellal Atlas. While the Beni Mousa plain shows a low fracture density due to the presence of quaternary deposits which mask the deep faults affecting the Cenozoic cover of this plain. In the piedmont of Beni Mellal, the junction zone between Beni Mellal Atlas and the Beni Moussa plain, the main directional peaks that predominate this transition zone are oriented E-W and ENE-WSW, they are inherited from Late Variscan period (Du Dresney, 1975; Mattauer et al., 1977).

### 3. Results and Discussion

The map of the reduced residual magnetic field to the pole (Figure 5) made it possible to distinguish several high and weak amplitudes anomalies,

characterized by an intensity values pair (high values in red to pinkish and weak values in blue). The observed magnetic signatures generally show a NE-SW to ENE-WSW and E-W trend in its orientation. To determine the geological sources of these magnetic anomalies, the geological map was superimposed with the magnetic data reduced to pole. In the western part of the study area, four geomorphological and structural zones have been identified; those zones correspond to two depressions and two high regions separated by major structural accidents (Figure 10). We distinguish from north to south: Beni Moussa plain (N1), the border zone of Afourer Atlas (P1, P2 and P3), Ait Attab syncline zone (N2) and the Ait Rhouja-Ait Seri zone (P4). The positive anomaly P1 reflects the magnetic signature of Ait Arki anticline occupied by the Triassic gypsum and basaltic formations. These formations have revealed at a depth of 1490 m in the KMS1 oil drilling, carried out near the Khemis Oulad Ayad locality (B.R.P.M., 1971).

The areas with high anomalies (P2, P3 and P4) are attributed to basaltic flows intercalated between

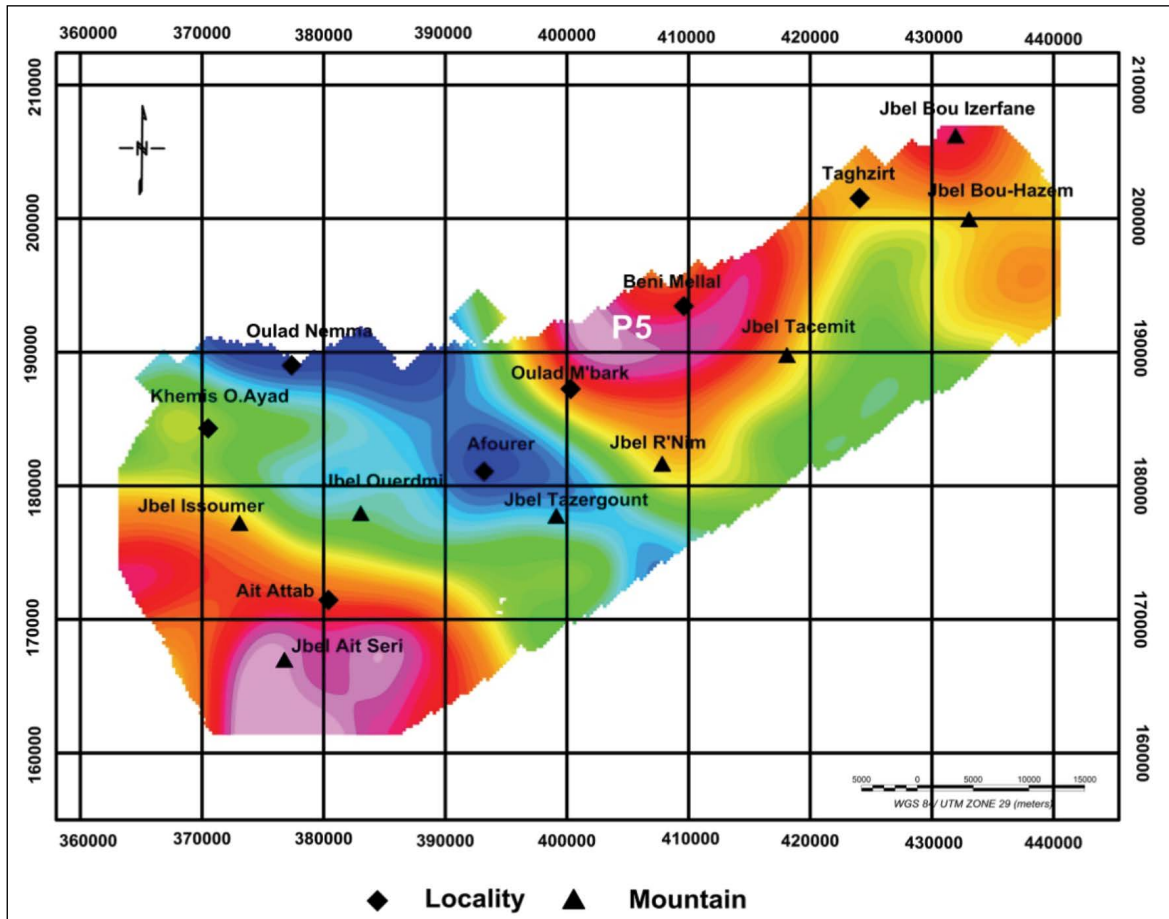


Figure 10- Upward continuation map for 4 km generated from RTP of residual magnetic field.

the mid-Jurassic “red beds” (Souhel 1996; Michard et al., 2011). These basaltic flows result from two middle Jurassic and early Cretaceous magmatic events (Monbaron 1981; Jenny et al., 1981) (Figure 5), that confirms to us these high magnetic anomalies are generated by these magnetic formations. In the eastern part of the study area, the geological outcrops are mainly presented by Liassic carbonates. The magnetic anomaly P5 does not seem to have a corresponding surface expression, thereby suggesting that its source is deeply buried. Indeed, this anomaly, whose the center is located in the west of Beni Mellal, persists to a continuation of 4 km, witnessing its deep origin (Figure 11).

The second anomaly P6, located at the western extremity of the study area appears to be correlated with the presence of Middle Jurassic magmatic intrusions in Taghzirt region and upper Triassic argillites in some locations (Rolley 1978; Haddoummi et al., 2010). The negative magnetic

anomalies N1, N2 and N3 correspond respectively, to the Quaternary cover of the Tadla plain, the Ait Attab syncline whose heart is occupied by the Cretaceous carbonate and terrigenous formations; finally; to the Liassic slab of the Atlas Afouer that overcomes the Beni Moussa plain. These formations are characterized by a weak magnetic susceptibility responsible for the low signature compared to previous ones.

The TDR map (Figure 6) has made it possible to identify the magnetic anomalies already detected by the reduced residual magnetic field map. The zero contour lines (inclination angle  $\theta = 0$ ) corresponds to geological contacts such as faults, fracture zones or lithological boundaries (Salem et al., 2008). Indeed, the projection of the Tilt derivative map on the geological map of the study area reveals the existence of a fault systems mainly oriented in ENE-WSW, E-W, N-S and NW-SE. Thoses directions characterize the Atlasic Chain evolution during Mesozoic and Cenozoic periods (Choubert and Faure-Muret, 1960-

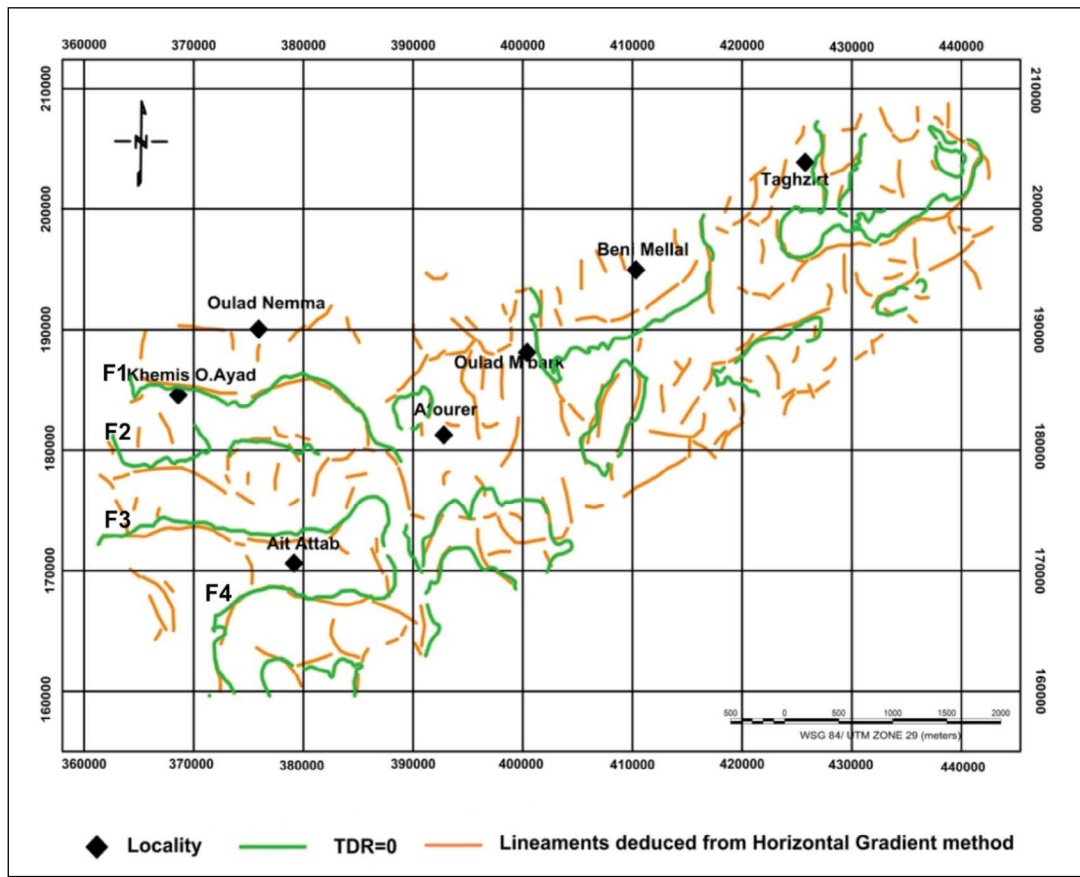


Figure 11- Magnetic lineaments map.

1962; Sadki, 1992; Zouine, 1993). We distinguish several major structures (Figure 11):

- Fault F1, named Beni Ayat border fault or the northern Atlasic fault, is an overlapping fault which constitute an abnormal contact with the deformed Mesozoic deposits of the Atlasic Chain (Afourer Atlas) on the cenozoic tabular layers of Tadla plain (Benzaquen, 1963, Du Dreseney, 1975; Mattauer et al., 1977) (Figure 3). Previous geological and structural studies (Rolley, 1973; Monbaron, 1982) have already revealed this fault. Its path draws a morphostructural and discontinuous line oriented E-W and hidden in some places by the Quaternary cover of Tadla plain. In Afourer Atlas, this fault is marked by argillites and altered basalts as outcrops of the upper Triassic (Ensslin, 1992);
- Fault F2 is called “Karia fault”, is delimited in the north by the Ait Imelloul block and in the south by that of Karia-Issoumer. This fault breaks the Karia syncline, which is reduced first to a pinch of Dogger

and upper Liassic before reappearing beyond this fault in the form of a depressed zone incorporated in the Middle Liassic, which obviously, towards the east becomes the Ait Imelloul syncline (Figure 3);

- Fault F3 is known in the literature by the Issoumer border fault (Du Dresnay, 1975; Souhel; Canerot, 1989). This is a major accident falls within a syndimentary extensional tectonic context which has controlled marine sedimentation during the Dogger and detrital deposition during the Bathonian (Souhel, 1996; Ibouh et al., 2000). This fault is responsible for the Ait Attab block tipping towards the West (Choubert, Faure-Muret, 1960-1962=; Jenney, 1984) (Figure 3). It was previously revealed by the seismic profile KT6 which extends from the Tadla plain in the North-West to the southern flank of the Ait Attab syncline in the South-East (Jabour and Nakayama, 1988; Hafid, 2006);

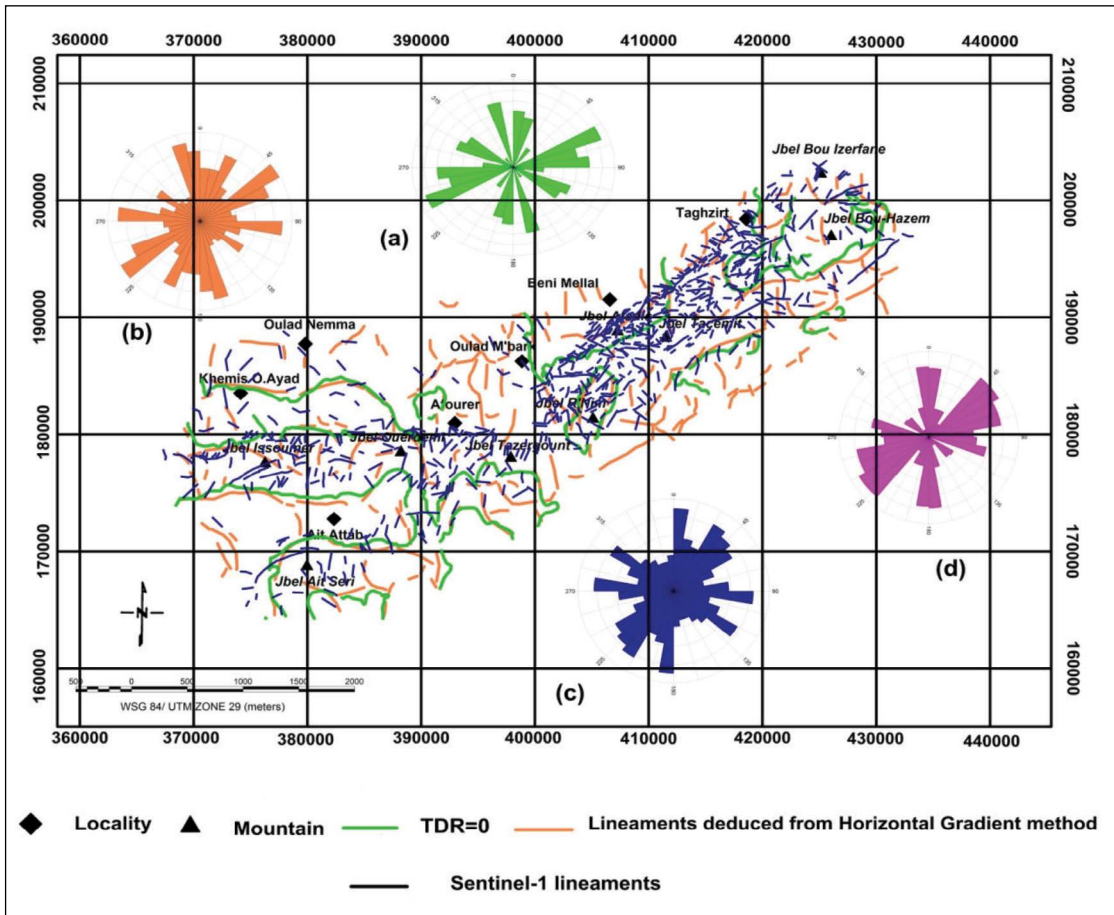


Figure 12- Fractures network map of the study area and rose diagram of highlighted directions obtained from: a) - TDR transformation; b) - Gradient horizontal method; c) – Sentinel-1 image; d) - field measurements.

- Fault F4 “Ait Seri Border Fault”: This reverse fault overlaps the lower and middle Liassic carbonate formations towards the north-west with the infra-Aptian red sandstones. Activated during lower and middle Liassic (Du Dresnay, 1972), this fault delimits the Ait Seri block (Figure 3) on which a reef-facies carbonate platform is deposited (Rolley, 1978).

In addition to major structures enhanced by the Tilt-angle transformation, several annex faults of these structures affect the study (Figure 11). The location of the local maxima from the horizontal gradient at various altitudes using reduced to pole aeromagnetic data facilitates the magnetic anomalies interpretation. Indeed, the horizontal gradient achieves local maxima over or near contacts separating two rock units with different magnetism (Fred et al., 2017). The alignment of these magnetic peaks reflects the geological discontinuities that can be interpreted in terms of faults or fractures.

The result obtained by the application of the horizontal gradient technique coupled to the upward continuation shows that the study area is controlled by four major families fractures trending NE-SW to ENE-WSW (N40-70°), E-W (N90-100°), N-S (N170-180°) and NW-SE (N130°) (Figure 12). These directions are associated with syn-sedimentary faults inherited from Pan-African and Hercynian Orogeny (Du Dresnay, 1975; Michard, 1976; Mattauer et al., 1977; Chorowicz et al., 1982; Piqué et al., 1998, 2007). In fact, during the upper Triassic-lower Cretaceous, these faults have controlled the opening and the subsidence of Atlasic basins in the form of rift basins by blocks tipping towards the north-west (Chorowicz et al., 1982; Chafiki, 1994 and Ensslin, 1992). The faults oriented N-S, have also been highlighted by horizontal gradient method, they are related to a submeridian compression phase relative to Alpine orogeny (upper Eocene-Quaternary) (Matteur et al., 1977; Monbaron, 1982; Morel et al., 2000). On



the other hand, the family of faults oriented NW-SE (N120-130°), are dimly represented in the study area. They are associated with transverse faulting showing a strike-slip character (Fadile, 1987; Chafiki, 1994; Souhel and Canerot, 1989). During middle Jurassic (Bajocian-Bathonian), these faults have reactivated to normal faults delineating the semi-grabens of high atlasic basin under the influence of an intense compression of WNW-ESE direction. The numerical processing of Sentinel 1-A image has provided similar results to those obtained from the airborne magnetic data analysis (Figure 12). The rose diagram reveals lineaments oriented N-S (N10 ° and N170-180 °); E-W (N90-100 °). NE-SW (N30-70°) and NW-SE (N120-130°) (Figure 12).

The Euler solutions obtained go hand in hand with the structure of lineaments deduced from the application of the horizontal gradient and TDR transformation (Figure 13). The depths obtained are between 0 and more than 1500 m. The lineaments

retraced by the Euler solutions are oriented mainly ENE-WSW to E-W and NW-SE.

The E-W trending lineaments display a depth exceeds 1500 m, which testify their deep origin. Those latter affect the anticlinal structures of Beni Mellal Atlas. During the Triassic-Jurassic period, the Ait Attab sector was submitted to an NW-SE extension by playing the faults oriented ENE-WSW to E-W to strike-slip faults. In the Afourer Atlas of Afourer, the Ait Attab syncline is bordered by two major faults: the Issoumer fault (F3) in the North-West and the Ait Seri fault (F4) in the South-East. Those two faults correspond to potential detachment levels of the Meso-Cenozoic cover. In fact, it is a “thin skin” cover characterized by a cover detachment at the base of the Triassico-Jurassic series and bordered by two ramp anticlines of “fault-bend fold” type (Issoumer and Ait Seri anticlines). The south-eastern flank of the Ait Attab syncline thrusts the Ait Seri anticline; with a liassic heart; through a back-thrust that probably

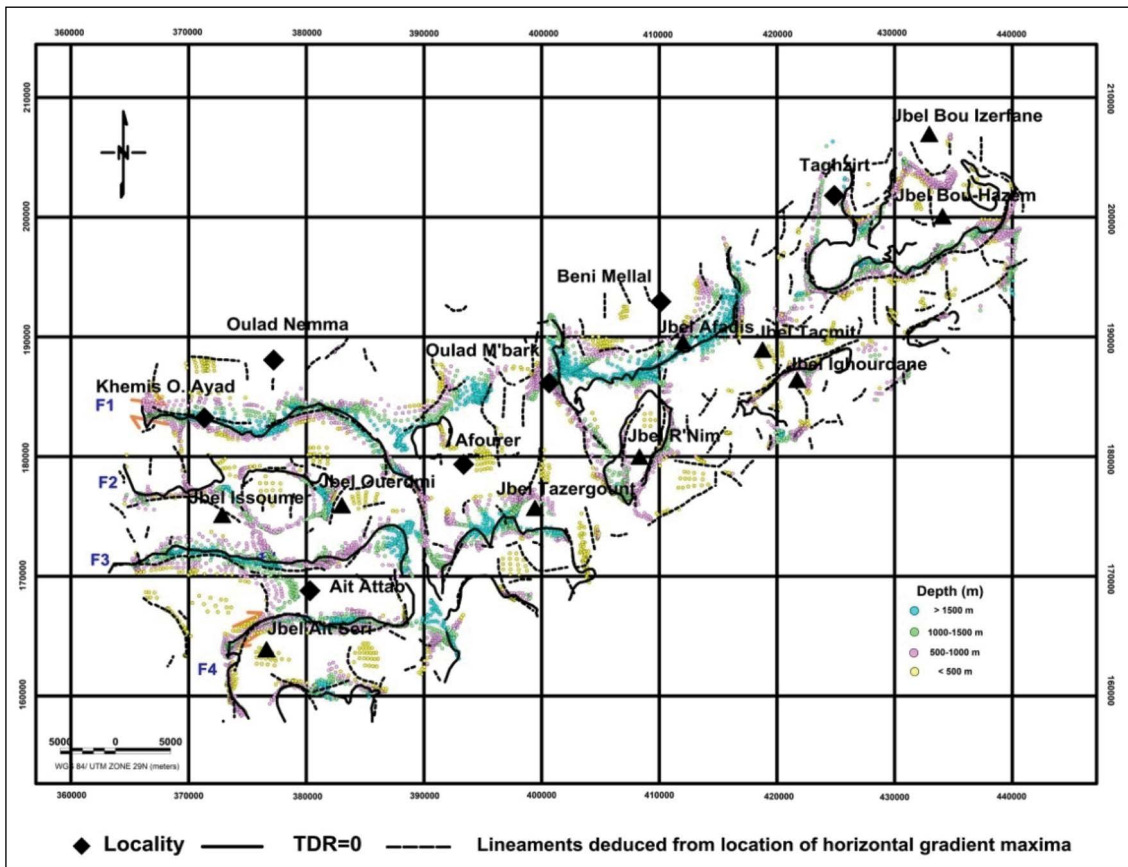


Figure 13- Superposition of Euler solutions and magnetic lineaments deduced from application of horizontal gradient and TDR transformation.

allows to compensate the blockage of overlap movement responsible for the advance of the detached sedimentary cover towards downstream (Beni Moussa plain). This overlap movement begins on the ramp detachment of the Ait Seri fault F4, after its blocking against the Cenozoic formations of Tadla plain, the faulting play was transferred in-depth on the ramp of Issoumer fault F3.

The magnetic lineaments obtained by the structural interpretation of aeromagnetic data are correlated with the lineaments extracted from the Sentinel 1-A radar image. The directional families of fractures measured in the field are mainly trending N10°, N40-75° and N170-180°. These directions merge with the karstic cavities developed on the lower Jurassic limestone of Beni Mellal Atlas (Bienfait, 1978). The fracture set trending N40-70° is related to Hercynian deformation which shows a brittle tectonic materialized by the replay of the major faults NE-SW.

#### 4. Conclusion

The current study relies on the fusion of aeromagnetic data as well as the radar remote sensing. It aims to define the directions of the main structural elements in Beni Mellal Atlas and to understand their tectonic origin. In fact, the map of the reduced to pole of residual magnetic field has allowed highlighting many magnetic anomalies of varying shapes, amplitudes and depths. From a geological view, the most important anomalies are matched with the presence of basaltic flows that resulted from two magmatic events during Bathonian and Lower Cretaceous. The use of tilt angle derivative (TDR), the horizontal gradient technique combined with the upward continuation (until 4 km) and the Euler deconvolution method has allowed highlighting magnetic alignments that correspond to faults. The most important ones are extended along the main structural accidents which are already recognized by classical geological studies (Monbaron, 1981; Rolley, 1973; Fadile, 1987). In fact, the TDR map made it possible to determine the major structural accidents that cross Beni Mellal Atlas (the border Atlasic fault, Issoumer fault, Ait Seri fault) and contribute to its subdivision into collapsed blocks. The NE-SW to ENE-WSW, E-W and N-S directions dominate magnetic faults trends that fit into the same directional families obtained from Sentinel image processing. The

major lineaments with the N40-70° direction represent normal synsedimentary faults, they are crosscut by the N-S (N170-180°) trending faults that are related to tectonic submeridian alpine compression (Matteur et al., 1977; Monbaron, 1981). These faults influenced the thickness variation of the sedimentary cover, which reflects a collapse movement of the basement relating to a synsedimentary distensive tectonics active since the Triassic to the lower Cretaceous.

The Euler solutions confirm and redraw, in general, the lineaments obtained by the magnetic data and Sentinel-1 image interpretation. The estimated depths vary between 0 m and more than 1500 m. The E-W trending lineaments display a depth exceeds 1500 m, which testify their deep origin. They affect the basic deposits of the Triassic layers and the Liassic carbonates, thus reflecting that the study area has undergone a thin-skinned deformation. Indeed, this paleo-stress field played a primordial role in the structuring of the Beni Mellal Atlas including a fourer Atlas whose presence of a major faults system allowed to divide the sector into collapsed blocks and tipped to the north-west. Below the Issoumer and Ait Seri faults, detachment ramps located at the base of the Lias and inside the Triassic serie are the cause of the Meso-Cenozoic cover detachment that comes to thrust towards the N-W the Atlasic border zone and the Cretaceous and Tertiary deposits of Tadla Plain. These structural results present a useful informations to guide hydrogeological prospecting campaigns in Beni Mellal Atlas.

#### Acknowledgements

We would like to thank the Applied Geology Division of the Ministry of Energy, Mines and Sustainable Development-Rabat, for providing the aeromagnetic data used in this study.

#### References

- Abderbi, J., Khattach, D. 2012. Apport des données aéromagnétiques et gravimétriques à l'étude de la structure géologique des Hauts Plateaux méridionaux, Maroc. *Journal of Hydrocarbons Mines and Environmental Research*. 2(2), 111-118. Amar, M. 2013.
- Adiri, Z., El Harti, A., Jellouli, A., Lhissou, R., Maacha, L., Azmi, M., Zouhair, M., Bachaoui, E.M. 2017. Comparison of Landsat-8, ASTER and Sentinel

- 1 satellite Remote Sensing data in Automatic Lineaments Extraction: a case study of Sidi Flah-Bouskour inlier, Moroccan Anti Atlas, *Advances in Space Research*, 60, 2355-2367.
- Alonso-Contes, C. A. 2011. Lineament mapping for groundwater exploration using remotely sensed imagery in a karst terrain : Rio Tanama and Rio de Arecibo basins in the northern karst of Puerto Rico. Master's Thesis, Michigan Technological University, 70p.
- Amar, M. 2013. Apport de l'analyse structurale et de la géophysique à la reconnaissance du système aquifère du Haut Atlas oriental, Maroc. Thèse doctorat, Université Moulay Ismail Meknès.
- Amar, M., Manar, A., Boualoul, M. 2012. Apport de la cartographie aéromagnétique à l'identification structurale du système aquifère des sources de l'Oasis de Figuig (Maroc). *Bulletin de l'Institut Scientifique, Rabat, section Sciences de la Terre*, 2012, 34, 29-40.
- B.R.P.M., 1971. Historique du sondage pétrolier de Khemis Oulad Ayad N°3000/36 (KMS1). Permis de Béni Moussa
- Bardon, C., Bossert, A., Hamzeh, R., Westphal, M. 1978. Paléomagnétisme des formations paléovolcaniques du Crétacé inférieur dans l'Atlas de Béni-Mellal (Maroc). *Notes Service et mémoire Géologique Maroc*, 39(272), 7-26.
- Beauchamp, J. 1988. Triassic sedimentation and rifting in the High Atlas (Morocco), in *Triassic-Jurassic Rifting: Continental Breakup and the Origin of the Atlantic Ocean and Passive Margins*, W. Mainspeizer, Elsevier Sci., New York, 447 – 497.
- Benzaquen, M. 1963. Bordure septentrionale de l'Atlas de Béni Mellal. Contribution à l'étude géologique de la région d'El Ksiba. *Notes et Mém. Serv. Géol. Maroc* 22(170), 20-45.
- Bienfait, P. 1978. Note relative aux cavités dans la région de Béni Mellal (Maroc). Direction de la région Hydraulique de Béni Mellal (D.R.H), 27p.
- Bouchaou, L. 1988. Hydrogéologie du bassin des sources karstiques du complexe calcaire haut atlasien du Dir de Béni Mellal (Maroc). Thèse Doctorat 3ème cycle. Univ. Franche Comté, 182p, Besançon.
- Boutirame, I., Boukdir, A., Akhsass, A., Boutirame, F., Manar, A., Aghzzaf, B. 2018. Contribution of gravity data and Sentinel-1 image for structural mapping. Case of Beni Mellal and Beni Moussa plain (Morocco). *E3S Web Conferences*, 37, 05002.
- Chafiki, D. 1994. Dynamique sédimentaire à l'articulation plate-forme - bassin : exemple du Lias de la région de Béni- Mellal (Haut-Atlas central, Maroc). Thèse 3ème cycle, Université Cadi Ayyad, 185 p, Marrakech.
- Charrière, A., Haddoumi, H., Mojon, P.O. 2005. Découverte du Jurassique supérieur et d'un niveau marin du Barrémien dans les « Couches rouges » continentales du Haut Atlas central marocain : implications paléogéographiques et structurales. *Comptes rendus Palevol*, 4, 385–394.
- Chorowicz, J., Alem, M., Bahmad, A., Chari, H., EL Kochri, A., Medina, F., Tamain, G. 1982. Les anticlinaux éjectifs du Haut Atlas : résultat de tectoniques atlasiques superposées. *C. R. Acad. Sci. Paris*, 294, 271-274.
- Choubert, G., Faure Muret, A. 1960-1962. Evolution paléogéographique et structurale des domaines méditerranéens et alpins d'Europe « Tome 1 ». Evolution du domaine atlasique marocain depuis les temps paléozoïques. *Mém. hors série, Soc. Géol. France*, 1, 447-527.
- Corgne, S., Magagi, R., Yergeau, M., Sylla, D. 2010. An integrated approach to hydro-geological lineament mapping of a semi-arid region of West Africa using Radarsat-1 and GIS. *Remote Sensing of Environment*, 114, 1863–1875.
- Dauteuil, O., Moreau, F., Qarqori, K. 2016. Structural pattern of the Saïss basin and Tabular Middle Atlas in northern Morocco: hydrological implications. *J Afr Earth Sci*, 119, 150–159.
- Debeglia, N. 2005. Estimation de la direction d'aimantation pour une réduction au pôle optimale du champ magnétique. *BRGM/RP-54059-FR*, 34 p.
- Du Dresnay, R. 1972. Les phénomènes de bordure des constructions carbonatées du Lias moyen du Haut Atlas central (Maroc). *C.R. Acad. Des Sc. Paris*, 275, 341-344, 535-537.
- Du Dresnay, R. 1975. Influence de l'héritage structural tardihercynien et de la tectonique contemporaine sur la sédimentation jurassique, dans le sillon marin du Haut- Atlas, Maroc. 9<sup>ème</sup> Congrès international de Sédimentologie, Nice, 103-108.
- Ejep, J.S., Olasehinde, P., Appollonia, A., Okunlola, I. 2017. Investigation of Hydrogeological Structures of Paiko Region, North-Central Nigeria Using Integrated Geophysical and Remote Sensing Techniques. *Geosciences*, 7, 122-140.
- El Gout, R., Khattach, D., Houari, M. R. 2009. Etude gravimétrique du flanc nord des Béni Snassen (Maroc nord oriental): implications structurales et hydrogéologique. *Bull. Ins Sci., Rabat, section Sciences de la Terre*, 31, 61-75.

- Ensslin, R. 1992. Cretaceous synsedimentary tectonics in the Atlas system of Central Morocco, *Geol. Rundsch.*, 81, 91-104.
- Everaerts, M., Mansy, J.L. 2001. Le filtrage des anomalies gravimétriques, une clé pour la compréhension des structures tectoniques du Boulonnais et de l'Artois (France), *Bulletin de la Société Géologique de France* 172, 3, 267–274.
- Fadile, A., 1987. Structure et évolution alpine du haut Atlas central sur la transversale Aghbala-Imilchil (Maroc). Thèse de 3<sup>ème</sup> cycle Univ. Paul Sabatier, 300p, Toulouse (no published).
- Fred, Y., Pérez, C., López-Loera, H., Fregoso-Becerra, E., Yutsis, V., Martínez-Ruiz, V.J., Dávila-Harris, P. 2017. Caracterización de lineamientos estructurales y sus implicaciones hidrogeológicas en la cuenca de Villa Hidalgo (San Luis Potosí) integrando métodos geofísicos potenciales. *Boletín de la Sociedad Geológica Mexicana*, 69 (3), 555 – 576.
- Guezal, J., El Baghdadi, M., Barakat, A. 2013. Les Basaltes de l'Atlas de Béni-Mellal (Haut Atlas Central, Maroc) : un Volcanisme Transitionnel Intraplaque Associé aux Stades de L'évolution Géodynamique du Domaine Atlasique. *Anuário do Instituto de Geociências*, 36 (2), 70-85.
- Haddoumi, H. 1988. Les Couches rouges (Bathonien à Barrémien) du synclinal des Aït Attab (Haut Atlas central, Maroc) ; étude sédimentologique et stratigraphique. Thèse de 3<sup>ème</sup> cycle, Université de Nancy I, 133 p.
- Haddoumi, H., Charrière, A., Mojon, P.O. 2010. Stratigraphie et sédimentologie des « Couches rouges » continentales du Jurassique-Crétacé du Haut Atlas central (Maroc) : implications paléogéographiques et géodynamiques. *Comptes rendus Geobios*, 43, 431-451.
- Hafid, M. 2006. Styles structuraux du Haut Atlas de Cap Tafelney et de la partie septentrionale du Haut Atlas occidental: tectonique salifère et relation entre l'Atlas et l'Atlantique. *Notes et Mém. Serv. géol. Maroc*, 465, 172p.
- Hoepffner, C., Houari, M.R., Bouabdelli, M., 2006. Tectonics of the North African Variscides (Morocco, Western Algeria), an outline, in Frizon de Lamotte D., Saddiqi O., Michard A. (Eds.), *Recent Developments on the Maghreb Geodynamics*. *C. R. Geosci.* 338, 25-40.
- Hobbs, W.H. 1912. *Earth features and their meaning: an introduction to geology for the student and the general reader*. Macmillan, New-York, 506 p.
- Ibouh, H., Chafiki, D., Bouabdelli, M., Souhel, A., El Bchari, F., Elhariri, K.H., Canerot, J. 2000. Rôle de la tectonique distensive du Toarcien inférieur dans l'évolution de la chaîne haut-atlasique centrale du Maroc. *Strata*, 1, 10, 103-105.
- Jabour, H., Nakayama, K. 1988. Basin modeling of Tadla basin, Morocco, for hydrocarbon potential, *AAPG bull.*, 72, 1059-1073.
- Jenny, J., Le Marrec A., Monbaron, M. 1981. Les Couches rouges du Jurassique moyen du Haut Atlas central (Maroc) : corrélations lithostratigraphiques, éléments de datations et cadre tectono-sédimentaire. *Bull. Soc. Géol. France*, 23, 6, 627–639.
- Khamis, M., Basheer, A., Rabeih, T., Khalil, A., Essam Eldin. A. A., Sato, M. 2014. Geophysical assessment of the hydraulic property of the fracture systems around Lake Nasser-Egypt: in sight of polarimetric borehole radar. *NRIAG Journal of Astronomy and Geophysics*, 3, 7-17.
- Lachaine, G. 1999. Structures géologiques et linéaments, Beauce (Québec). Mémoire de maîtrise, Département de géographie et de télédétection, Université de Sherbrooke, 83 pp.
- Laville, E., Harmand, C. 1982. Évolution magmatique et tectonique du bassin intracontinental mésozoïque du Haut Atlas (Maroc) : un modèle de mise en place synsédimentaire de massifs "anorogéniques" liés à des décrochements, *Bull. Soc. géol. Fr.*, XXIV, 2, 213–227.
- Lee, J. S., Grunes, M. R., et de Grandi, G., 1999. Polarimetric SAR speckle filtering and its implication for classification. *IEEE Transactions on Geoscience and Remote Sensing*, 37, 2363–2373.
- Mansour, M., Ait Brahim, L. 2005. Apport de la Télédétection radar et du MNT à l'analyse de la fracturation et la dynamique des versants dans la Région de Bab-taza, Rif, Maroc. *Télédétection*, 5, 95-103.
- Mattauer, M., Tapponier, P., Proust, F. 1977. Sur les mécanismes de formation des chaînes intracontinentales. L'exemple des chaînes atlasiques du Maroc. *Bull. Soc. Géol. France*, 19, 521-526.
- Michard, A. 1976. *Élément de géologie marocaine*. Éditions du service géologique du Maroc, Note et Mém., 252.
- Michard, A., Saddiqi, O., Chalouan, A., Rjimati, E., Mouttaqi, A. 2011. In *Nouveaux Guides géologiques et miniers du Maroc / New Geological and Mining Guidebooks of Morocco*. Notes et Mémoires du Service géologique du Maroc, 556-564.
- Miller, H.G., Singh, V. 1994. Potential field tilt – a new concept for location of potential field sources; *J. Appl. Geophys.* 32, 213–217.



- Monbaron, M. 1981. Sédimentation, tectonique synsédimentaire et magmatisme basique l'évolution paléogéographique et structurale de l'Atlas de Béni Mellal (Maroc) au cours du Temps Mésozoïque, ses incidences sur la tectonique atlasique. *Ecologia Géol. Helv*, 74(3), 625-638.
- Monbaron, M. 1982. Précisions sur la chronologie de la tectogénèse atlasique. *C.R. Acad. Sc. Paris* : t. 294, 2, 883-885.
- Monbaron, M. 1985. Carte géologique du Maroc au 1/100 000ème, feuille Béni Mellal. *Notes et Mém. Serv. Géol. Maroc*, no: 341.
- Moreau, F., Gibert, D. et Saracco, G. 1996. Filtering non-stationary geophysical data with orthogonal wavelets, *Geophysical Research Letter*, 23, 407-410.
- Morel, J.L., Zouine, E.M., Andrieux, J., Faure-Muret, A. 2000. Déformations néogènes et quaternaires de la bordure nord haut-atlasique (Maroc) : rôle du socle et conséquences structurales. *Journal of African Earth Sciences*, 30, 119-131.
- Oruc, B., Selim H. 2011 Interpretation of magnetic data in the Sinop area of Mid Black Sea, Turkey, using tilt derivative, Euler deconvolution, and discrete wavelet transform; *J. Appl. Geophys.* 74 194–204.
- Piqué, A., Aït Brahim, L., Aït Ouali, R., Amrhar, M., Charroud, M., Gourmelen, C., Laville, E., Rekhiss, F., Tricart, P. 1998. Évolution structurale des domaines atlasiques du Maghreb au Méso-Cénozoïque ; le rôle des structures héritées dans la déformation du domaine atlasique de l'Afrique du Nord. *Bull. Soc. géol. France* 169, 6, 797–810.
- Piqué, A., Soulaïmani, A., Hoepffner, C., Bouabdelli, M., Laville, E., Amrhar, M., Chalouan, A. 2007. *Géologie du Maroc*. Editions GEODE, Marrakech.
- Ranganai, R.T., Ebinger, C.J. 2008. Aeromagnetic and Landsat TM Structural Interpretation for identifying regional groundwater exploration targets, south-central Zimbabwe Craton. *J. Appl. Geophys.*, 65, 73–83.
- Reid, A. B., Allsop, J.M., Granser, H., Millet, A. J., Somerton, I.W. 1990, Magnetic interpretation in three dimensions using Euler deconvolution: *Geophysics*, 55, 80–91.
- Rolley, J.P. 1973. Etude géologique de l'Atlas d'Afourer - Haut-Atlas central - Maroc. Stratigraphie. Thèse Doctorat 3ème cycle, Univ. de Grenoble, 100 p, Grenoble.
- Rolley, J.P. 1978. Carte géologique du Maroc au 1/100.000: feuille d'Afourer. Notice explicative. *Notes et Mémoires du Service Géologique du Maroc*, 247, 247 bis: 1-103.
- Sadki, D. 1992. Le Haut Atlas central (Maroc) – stratigraphie et paléontologie du Lias supérieur et du Dogger inférieur : dynamique du bassin et des peuplements. Thèse Doct. d'Etat; Univ. Cadi Ayyad, Marrakech, 331 p.
- Salem, A., Williams, S., Fairhead, J.D., Smith, R., Ravat, D.J. 2008. Interpretation of magnetic data using tilt-angle derivatives; *Geophysics*, 73, L1–L10.
- Souhel, A. 1996. Le Mésozoïque dans le Haut Atlas de Béni-Mellal (Maroc). Stratigraphie, sédimentologie et évolution géodynamique. Mémoire de Thèse d'État, Université Caddi Ayad, 235 p, Marrakech.
- Souhel, A., Canerot, J. 1989. Polarités sédimentaires téthysienne puis atlantique : l'exemple des couches rouges jurassico-crétacées du Haut-Atlas central (Maroc). *Sci. Géol., Mém.*, 84, 39-46.
- Srivastava, P.K., Bhattacharya, A.K. 2006. Groundwater assessment through an integrated approach using remote sensing, GIS and resistivity techniques: A case study from a hard rock terrain. *Int. J. Rem. Sens.*, 27, 4599–4620.
- Thompson, D.T., 1982. EULDPH: A new technique for making depth estimates from magnetic data: *Geophysics*, 47(1), 31–37.
- Van Senden, D.C., Portielje, R., Borer, A. 1990. Vertical exchange due to horizontal density gradients in lakes; the case of Lake Lucerne. *Aquatic Science*, 52p.
- Verset, Y. 1985. Carte géologique du Maroc au 1/100 000ème, feuille Kasba Tadla. *Notes et Mém. Serv. Géol. Maroc*, n°340.
- Ziegler, P., Cloetingh, S., Wees, J. 1995. Dynamics of intraplate compressional deformation: The Alpine foreland and other examples, *Tectonophysics*, 252, 7 – 60.
- Zouine, El. 1993. Géodynamique récente du Haut Atlas. Evolution de sa bordure septentrionale et du Moyen Atlas sud-occidental au cours du Cénozoïque. *Doct. Etat, Es-Sc. Nat. Univ. Mohamed 5 Fac. Sciences*, 330 p, Rabat (unpublished).

